

General features of latent track formation in magnetic insulators irradiated with swift heavy ions

G. Szenes

Institute for General Physics, Eötvös University, Muzeum krt 6-8, H-1088 Budapest, Hungary

(Received 12 September 1994)

A thermal spike model is proposed for the analysis of latent track formation in insulators. The model predicts that above a threshold electronic stopping power S_{et} $R_e^2 \sim \ln S_e$ for $1 \leq S_e/S_{et} \leq 2.7$ followed by $R_e^2 \sim S_e$ for $2.7 \leq S_e/S_{et}$ (R_e being the effective track radius). A simple expression is derived for the evaluation of S_{et} from material parameters. A good agreement is found with literature data on latent tracks in magnetic insulators. The analysis showed that the width of the temperature distribution is $a(0) = (4.5 \pm 0.25)$ nm and the energy deposited in the spike is $0.17S_e$.

The application of the thermal spike model to irradiation phenomena is an old idea.¹ However, even in the most elaborate models^{2,3} rather rough approximations must be used to derive expressions suitable for comparison with experiments. In the present paper a phenomenological approach is reported promising significant progress.

Swift heavy ions induce amorphization in many crystalline insulators. The amorphous phase along the ion trajectory is called the latent track. The observation was made 35 years ago on mica by electron microscopy.⁴ Later Sigrist and Balzer⁵ showed that the formation of latent tracks is related to the electronic stopping power of energetic ions, S_e . Till now, the theories based on the Coulomb explosion and thermal spike models could not lead to quantitative predictions and even to useful correlation (for a review, see Refs. 6 and 7). We demonstrate the possibilities of our approach by the analysis of the amorphization observed along the ion trajectories in insulators. In these measurements the experimental quantity—the effective radius of the amorphized cylinder R_e —can be simply related to the parameters of the thermal spike. Besides some solid-state nuclear track detectors, where the first step in the detection process is the formation of a similar latent track, the results may be also useful for the interpretation of the experiments on electronic sputtering,⁸ ion-beam-induced deformation in amorphous materials,⁹ and defect formation and annealing in crystalline materials related to the electronic stopping power S_e of energetic ions.^{10,11}

First a brief review of the present model¹² is given followed by the analysis of the experimental data published in the literature on latent track formation in magnetic insulators and the discussion. The basic assumption of all thermal spike models is that around the trajectory of the high-energy ion a high-temperature region is formed in the material. In the following, all temperatures refer only to the phonon system. It is assumed that when the temperature exceeds the melting point of the crystal a melt is formed. Due to its small diameter, the cooling rate of the melt may reach 10^{13} – 10^{14} K/s that results in an amorphous structure when the melt solidifies.

The peak temperature of the spike T_p first grows up to its maximum value within a very short time ($< 10^{-12}$ s) and then it decreases and the spike broadens as a result of heat conduction. We shall measure the time t from that moment when T_p is the maximum in the phonon system. Let us denote by T_{ig} , T_m , $T(r, t)$ the target temperature, the melting point, and the temperature at a distance r from the ion trajectory, respectively. If $\Delta T(r, t)$ is the temperature increase in the thermal spike then $T(r, t) = T_{ig} + \Delta T(r, t)$. One of the main assumptions of our model is that $\Delta T(r, t)$ can be approximated by a Gaussian distribution:

$$\Delta T(r, t) = Q [\pi a^2(t)]^{-1} \exp\{-r^2/a^2(t)\}, \quad (1)$$

where $a^2(t)$ depends on thermal diffusivity. The value of Q can be obtained from the balance of energy $Q = (gS_e - L\rho\pi R^2)(\rho c)^{-1}$, where gS_e is the fraction of energy deposited in the thermal spike, $R = R(t)$ is the radius of the melted zone, c , ρ , and L are the mean specific heat, the density, and the latent heat of phase transition, respectively. In the following, the approximation $gS_e \gg L\rho\pi R^2$ will be used. This is usually valid for materials in which latent track formation can be observed.

A second assumption of the model is that the volume of the amorphous phase formed along the ion trajectory is proportional to the maximum volume of the melt. In the following, the proportionality factor is taken equal to 1. This amorphous phase has been observed by different physical methods in many irradiated insulators.⁷

To reach the melting point the temperature in the thermal spike should be increased by $T_0 = T_m - T_{ig}$. The size of the melted region may increase or decrease as the thermal spike broadens. The maximum value $R = R_0$ can be obtained from the condition $dr/dt = 0$ at $\Delta T = T_0$. A short calculation leads to a very simple result: if the temperature at $r = a(t)$ is denoted by T_a , then $R = R_0$ when $T_a = T_0$. The width of the temperature distribution $a(t)$ monotonically increases and T_a decreases with time in the cooling spike. If initially $T_0 > T_a$ at $t = 0$ [$R(0) < a(0)$], then $T_0 = T_a$ never fulfills and the melted zone will have its maximum diameter at $t = 0$. If

$T_0 < T_a$ at $t=0$ [$R(0) > a(0)$] then the melted zone expands up to $t=t'$ when $T_0 = T_a$ [$R_0 = R(t') = a(t')$] and further it shrinks for $t > t'$. The two behaviors are described by expressions, obtained from Eq. (1) by introducing the conditions for maximum (for details, see Ref. 12):

$$R_0^2 = a^2(0) \ln(S_e/S_{et}), \quad 2.7 \geq S_e/S_{et} \geq 1, \quad (2a)$$

$$R_0^2 = [a^2(0)/2.7](S_e/S_{et}), \quad S_e/S_{et} \geq 2.7, \quad (2b)$$

$$S_{et} = \rho \pi c a^2(0) T_0 / g. \quad (3)$$

Thus, the track radius and the electronic stopping power are related through two remarkably simple equations. According to Eq. (2a) at low electronic stopping power there is a threshold S_{et} below which no amorphization is predicted. At this point $T_p = T_0$. Equation (2a) describes a logarithmic variation of the damage cross section $A = \pi R_0^2$ in the $1 < S_e/S_{et} < 2.7$ range. Expression (2b) is an equation of a straight line for $S_e/S_{et} > 2.7$ going through the origin. There is a smooth transition between the logarithmic and linear regimes. At $S_e = 2.7S_{et}$, Eqs. (2) provide the same value for R_0^2 . The g parameter does not figure explicitly in Eqs. (2). It affects the variation of R_0^2 through S_{et} . The slopes of the linear and logarithmic expressions differ only in a numerical factor. This is an additional requirement of the model besides the threshold behavior and the existence of a logarithmic and a linear regime.

Since R_0 is obtained from a maximum condition, Eqs. (2) do not contain the time as a variable. Whatever is the time interval, short or long, necessary to reach the maximum size of the melted zone, it does not affect R_0 . This is the reason why thermal diffusivities do not figure explicitly in the equations, which is a great advantage of the model. The parameter which is related to thermal diffusivities is $a(0)$. However, it can be obtained from fitting.

In the present form of the model T_m and L are equilibrium values. However, due to the short lifetime of the thermal spike ($\sim 10^{-11}$ s) the actual and equilibrium values may differ. Pulsed-laser experiments may provide independent quantitative information that can be taken into account in Eqs. (2) and (3).

As a result of systematic studies of French teams at the GANIL accelerator (Caen, France) at present experimental data on latent track radii R_e due to ion bombardment have been published on yttrium iron garnet (YIG),¹³ $\text{BaFe}_{12}\text{O}_{19}$,^{14,15} $\text{SrFe}_{12}\text{O}_{19}$,¹⁶ MgFe_2O_4 ,¹⁷ NiFe_2O_4 ,¹⁸ ZnFe_2O_4 ,¹⁹ and some additional results are given in Ref. 20. No more latent track data suitable for our analysis have been published so far for any other material. Therefore, the choice of magnetic insulator in the present study is not a deliberate restriction of our analysis to a special class of materials.

The latent track diameters were deduced from the variation of Mössbauer spectra due to amorphization under room-temperature ion bombardment. In Fig. 1 R_e^2 data are plotted versus $\ln(S_e/S_{et})$ ($R_e = R_0$ according to our second assumption) and the figure evidently suggests to apply Eq. (2a). The S_{et} values are not equal to the values

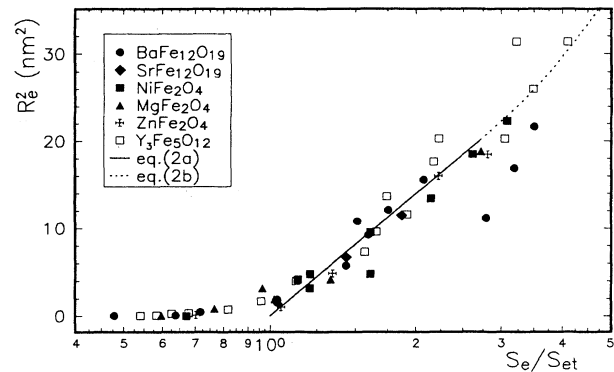


FIG. 1. Variation of track size versus S_e normalized to the threshold value S_{et} .

given in the original publications, because their magnitude depends on the function which is used in the extrapolation to $R_e = 0$. We used Eqs. (2a) and S_{et} was obtained for each material from the fit to the data by a least-squares procedure. Only data in the logarithmic regime were used in the fit. In a second step all data were plotted on a normalized S_e/S_{et} scale and the mean $a(0)$ value was obtained by the least-squares method.

It was reported by Meftah *et al.*¹³ that in YIG the damage cross sections are systematically higher for low ion velocities compared to the case of high ion velocities. The discussion of this problem based on the thermal spike model will be given in a separate publication.²¹ In the present analysis only the high-velocity data were used ($E > 7.6$ MeV/nucleon).

Compared to the typical error (20%) the deviation from the theoretical curve in Fig. 1 is not large except some points for $\text{BaFe}_{12}\text{O}_{19}$ obtained with U and Pb beams with very high electronic stopping power. However, the rest of the data for this material also nicely follow the theoretical curve. Since the large scatter of data starts above the logarithmic regime ($S_e/S_{et} > 2.7$), it does not affect the determination of S_{et} and of the slope. We do not believe that the origin of these deviations is related to physical reasons that ought to be taken into account in the analysis.

The threshold and logarithmic regimes can be easily recognized in Fig. 1. The linear regime starts at $S_e/S_{et} = 2.7$. Unfortunately the scatter is high in this range, thus the linear regime is not well represented in this plot. The existence of the linear regime is exhibited much better in the analysis of latent tracks in YIG irradiated with low-velocity ions, since in that case the majority of data belongs to the linear regime.²¹

The variation of the damage cross section versus S_e closely follows the same trend in all cases. This may be the result of the variation of $a(0)$ in different materials in a very narrow range which is undetected due to experimental errors. A second possibility is that $a(0) = \text{const}$ in Fig. 1 and the deviations from the master curve are related to experimental error. Our opinion is that the analysis of fine details would require higher precision and more data. Therefore, we conclude from the present data set

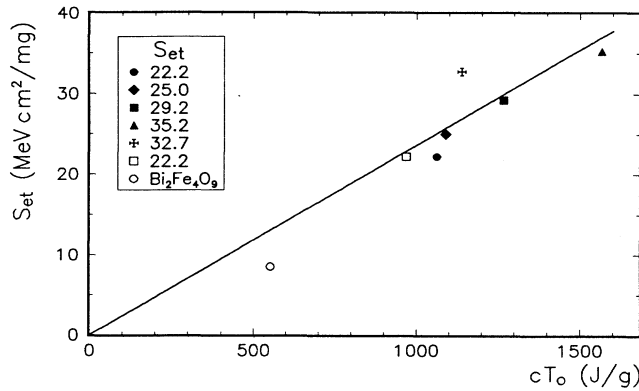


FIG. 2. Variation of S_{et} with material parameters. See Fig. 1 for legend. The $\text{Bi}_2\text{Fe}_4\text{O}_9$ point was not used in the fit.

that within the experimental error the initial width of the temperature distribution is identical in these magnetic insulators with $a(0) = (4.5 \pm 0.25)$ nm. Our description is phenomenological. The microscopic transient thermodynamic model³ may be more suitable to reveal the microphysical origin of this observation.

At $R_e^2 \leq 4$ nm² the deviation from the straight line in Fig. 1 is higher than the experimental error. This may be connected with the changing morphology of the tracks.¹³ At $R_e^2 \leq 4$ nm² the amorphous regions are isolated and approximately spherical. Our calculations were based on a cylindrical geometry which appears only at $R_e^2 > 4$ nm². Another source of deviation may be the incongruent melting of some materials.

An important assumption of the model is that the volume of the melt is proportional to that of the amorphous phase and the proportionality factor $k = 1$. The normalized plots in Fig. 1 prove that $k = \text{const}$ for magnetic insulators within the experimental error. In the opposite case the variation of k would affect the derived $a^2(0)$ values. This would give rise to a systematic separation of the damage cross sections which is not seen in the figures.

If the master curve for a certain class of materials is known then a single experimental point is sufficient to evaluate the variation of the damage cross section in the full range of S_e . For example, $\text{Bi}_2\text{Fe}_4\text{O}_9$ was irradiated at 77 K with 3.1-GeV Xe beam corresponding to $S_e \approx 34$ MeV cm²/mg (the precise value is not given). The track size was measured by Mössbauer spectroscopy,²² providing $R_e = (5.5 \pm 0.5)$ nm for the latent track radius. From the master curve in Fig. 1, we see that it corresponds to $S_e/S_{et} = 4.06$ giving $S_{et} = 8.4$ MeV cm²/mg. Now having this value the track radius at any S_e can be evaluated by Eqs. (2). Certainly, the accuracy of the estimate, to a large extent, depends on the error of the initial data.

Equation (3) offers a simple expression for the calculation of the threshold value of electronic stopping power

for track formation. According to Eq. (3) there is a linear relation between S_{et} and cT_0 . The plot in Fig. 2 confirms this relationship providing $a^2(0)/g = 120$ nm² and $g = 0.17$. For materials with incongruent melting the arithmetic average of the liquids and solidus temperatures T_{im} estimated from the appropriate phase diagrams^{23,24} were used for the calculation of T_0 . For $\text{SrFe}_{12}\text{O}_{19}$ we obtained $T_{im} = 1740$ K by a differential scanning calorimetry (DSC) measurement. The specific heat was calculated by the Dulong-Petit law. The low S_{et} estimated for $\text{Bi}_2\text{Fe}_4\text{O}_9$ from a single experimental point (omitted in the fit) is in agreement with other data in Fig. 2 [$T_m = 1233$ K (Ref. 20)].

We also measured the latent heat of phase transition in $\text{BaFe}_{12}\text{O}_{19}$ ($L = 240$ J/g) and $\text{SrFe}_{12}\text{O}_{19}$ (210 J/g) by high-temperature calorimetry. The average value of $L\rho\pi R^2(gS_e)^{-1}$ was found to be about 4% for $0 < R_0 < a(0)$ and it was assumed that this is typical for the rest of the magnetic insulators, as well. Thus we feel justified in using the approximation $gS_e \gg L\rho\pi R^2$ in the derivation of Eqs. (2), since the typical experimental errors of S_e and R_e^2 are about 20% (Refs. 13–20).

The validity of Eq. (3), the logarithmic variation of R_e versus S_e and the identical $a(0)$ and g values obtained for different magnetic insulators confirm the applicability of the thermal spike model to the problem of latent track formation in insulators. We emphasize that so far the threshold electronic stopping power for latent track formation could not be predicted by any theory. The correct description of the evolution of track radius with S_e has not been given so far by any versions of the Coulomb explosion or the thermal spike models. The present model can quantitatively account for the phenomenon. The temperature dependence—related to the variation of cT_0 —is also correctly reproduced.²¹

Systematic latent track studies have been also published on SiO_2 (Ref. 25) and mica.^{26,27} However, the R_e^2 - S_e relation is not unambiguous in these cases and additional data are required. Estimates based on the analysis of the available experimental result on SiO_2 , mica and also for some other materials suggest that the variation of $a(0)$ for magnetic and nonmagnetic insulators may be restricted to a rather narrow range.

The author is grateful to Dr. M. Toulemonde for stimulating discussions and offering his unpublished data for analysis. It is also a pleasure to thank Dr. F. Studer for supplying the specimens for the DSC measurements. This work was carried out in CIRIL (Caen, France) during which the author was supported by the Commission of the European Communities as part of the European Economic Community mobility action. The calorimetric measurements were made by a SETARAM DSC equipment purchased with the support of the Hungarian National Scientific Research Fund under Contract No. A062.

- ¹F. Seitz and J. F. Koehler, in *Solid State Physics: Advances in Research and Applications*, edited by F. Seitz and D. Turnbull (Academic, New York, 1956), Vol. 2, p. 305.
- ²L. T. Chadderton and I. M. Torrens, *Fission Damage in Crystals* (Methuen, London, 1969).
- ³M. Toulemonde, C. Dufour, and E. Paumier, *Phys. Rev. B* **46**, 14 362 (1992).
- ⁴E. C. M. Silk and R. S. Barnes, *Philos. Mag.* **4**, 970 (1959).
- ⁵A. Sigrist and R. Balzer, *Helv. Phys. Acta* **50**, 49 (1977).
- ⁶R. L. Fleischer, P. B. Price, and R. M. Walker, *Nuclear Tracks in Solids* (University of California Press, Berkeley, 1975).
- ⁷M. Toulemonde, S. Bouffard, and F. Studer, *Nucl. Instrum. Methods Phys. Res. Sect. B* **91**, 108 (1994).
- ⁸L. A. Baranov, Yu. V. Martynenko, S. O. Cepelevich, and Yu. N. Javlinkij, *Sov. Phys. Usp.* **156**, 477 (1988).
- ⁹S. Klaumünzer and G. Schumacher, *Phys. Rev. Lett.* **51**, 1987 (1983).
- ¹⁰A. Dunlop and D. Lesueur, *Mater. Sci. Forum* **97-99**, 553 (1992).
- ¹¹A. Iwase, S. Sasaki, and T. Iwata, *Phys. Rev. Lett.* **58**, 2450 (1987).
- ¹²G. Szenes, *Mater. Sci. Forum* **97-99**, 647 (1992).
- ¹³A. Meftah *et al.*, *Phys. Rev. B* **48**, 920 (1993).
- ¹⁴A. Meftah *et al.*, *Nucl. Instrum. Methods Phys. Res. Sect. B* **59/60**, 605 (1991).
- ¹⁵F. Studer *et al.*, *Radiat. Eff. Defects Solids* **116**, 59 (1991).
- ¹⁶C. Houpert *et al.*, *Nucl. Tracks Radiat. Meas.* **19**, 85 (1991).
- ¹⁷M. Toulemonde (private communication).
- ¹⁸M. Toulemonde and F. Studer, *Solid State Phenomena* **30/31**, 477 (1993).
- ¹⁹F. Studer *et al.*, *Nucl. Instrum. Methods Phys. Res. Sect. B* **82**, 91 (1993).
- ²⁰C. Houpert, Ph. D. thesis, University of Caen, 1989.
- ²¹G. Szenes (unpublished).
- ²²D. Groult, M. Hervieu, N. Nguyen, and B. Raveau, *J. Solid State Chem.* **76**, 248 (1988).
- ²³T. R. McGuire and E. L. Boyd, in *Magnetic and Other Properties of Oxides and Related Compounds, Numerical Data and Functional Relationships in Science and Technology*, edited by K. H. Hellwege and A. M. Hellwege, Landolt-Börnstein, New Series, Group III, Vol. 4b (Springer-Verlag, Berlin, 1970), p. 75; C. J. Kriessman and A. P. Greifer, *ibid.*, p. 216; V. J. Folden, *ibid.*, p. 315; H. P. J. Wijn, *ibid.*, p. 547.
- ²⁴H. J. Van Hook, *J. Am. Ceram. Soc.* **45**, 162 (1962).
- ²⁵A. Meftah, Ph. D. thesis, University of Caen, 1993.
- ²⁶R. Spohr, P. Armbruster, and K. Schaupert, *Radiat. Eff. Defects Solids* **110**, 27 (1989).
- ²⁷S. Bouffard, J. Cousty, Y. Pennec, and F. Thibaudau, *Radiat. Eff. Defects Solids* **126**, 225 (1993).